minerals

MDPI

Article

Gemology, Mineralogy, and Spectroscopy of an Attractive Tremolitized Diopside Anorthosite Gem Material from the Philippines: A New Type of Material with Similarities to Dushan Jade

Xiaomeng Ye, Feng Bai *, Manyu Li and Hao Sun

School of Gemmology, China University of Geosciences (Beijing), Beijing 100083, China; 2009190004@cugb.edu.cn (X.Y.); 2009160022@cugb.edu.cn (M.L.); 2109160003@cugb.edu.cn (H.S.)
* Correspondence: baifeng@cugb.edu.cn

Abstract: In recent years, a new type of material called Philippines "Dushan jade" has appeared in the gemstone market in China. This new type of material, very similar in appearance and physical properties to Dushan jade, an important ancient jade with a long history in China, is causing confusion in the market and poses identification difficulties. Microscopy, electron probe microanalysis, Fourier transform infrared (FTIR) spectroscopy, Raman microprobe spectroscopy, and ultraviolet-visible (UV-Vis) spectroscopy were used to study the gemology, mineralogy, and spectroscopy of rock samples from the Philippines in order to differentiate them from Dushan jade. The studies showed that Philippines rock is composed mainly of anorthite and minor amounts of diopside, tremolite, uvarovite, titanite, chromite, zoisite, prehnite, thomsonite-Ca, and chlorite, among which uvarovite, diopside, and tremolite are the main color causing minerals. The origin of the color is related to the electronic transitions involving Cr^{3+}, Fe^{2+}, Fe^{3+}, and charge transfer between the ions. The paragenetic mineral formation sequence of Philippines rock can be divided into three stages: (1) the magmatic stage: anorthite phenocryst, diopside, chromite, and titanite are formed first in the magma; (2) the metamorphic stage: anorthite phenocryst undergo fracture and recrystallization; the early fluid intrusion transforms diopside into tremolite forming uvarovite-grossular-andradite solid-solution around the anorthite and chromite; and (3) the late hydrothermal stage: the late hydrothermal solution fills in fractures with prehnite, thomsonite-Ca, and zoisite being formed. From the comparison studies, it was established that Philippines rock and Dushan jade are two completely different type of material. Philippines rock should be called "tremolitized diopside anorthosite".

Keywords: tremolitized diopside anorthosite; uvarovite; mineralogy; microscopy; spectroscopy

Citation: Ye, X.; Bai, F.; Li, M.; Sun, H. Gemology, Mineralogy, and Spectroscopy of an Attractive Tremolitized Diopside Anorthosite Gem Material from the Philippines: A New Type of Material with Similarities to Dushan Jade. *Minerals* **2021**, *11*, 152. https://doi.org/10.3390/min11020152

Academic Editors: Ferdinando Bosi and Thomas Hainschwang
Received: 28 December 2020
Accepted: 28 January 2021
Published: 31 January 2021

1. Introduction

Jades are generally separated into two groups in mineralogy: nephrite jade and jadeite jade. In Chinese gem market, however, jades are the fine grained rocks, which have beautiful appearance, durability, rarity, and technological value [1–4]. Dushan jade is characterized by the presence of saturated colors and its delicate texture. Dushan jade, nephrite jade, serpentine jade, and turquoise jade are known as the "four great jades" of China. The mining history can be traced back to the Neolithic Age, and it is the only zoisitized anorthosite used as a gem material in the world up to now [5–10]. In recent years, a new type of material, called Philippines "Dushan jade" by gemstone dealers has appeared on the Chinese gem market. The new material is very similar to Dushan jade in appearance and physical properties, causing confusion in the market and difficulties in identification, especially for the green variety of rock. At present, few studies have been undertaken on Philippines rock, and only the green rock variety has been studied via Raman microprobe spectroscopy, infrared spectroscopy, and ultraviolet-visible (UV-Vis)

spectroscopy [11,12]. Other colors of this rock have not been studied. In this research, representative samples of all color varieties of Philippines rock have been collected in order to conduct a systematic study on the gemology, mineralogy, and spectroscopy of the rocks with the aim of ascertaining the rock type and to differentiate the Philippines rock from Dushan jade, and hence be able to provide correct guidance to consumers.

2. Samples and Methods

In this study, eight representative samples covering all the color varieties of Philippines rock were selected, including white, green, cyan-gray, white with black spots, dark green, and brown (Figure 1). The refractive index (RI) and specific gravity (SG) of the samples were measured by the distant vison method and the hydrostatic weighing method, respectively [13,14]. The Vickers hardness (Hv) was measured by the Microvickers hardness tester and the values were converted to Mohs hardness values (H_M) by the expression $H_M = 0.675\sqrt[3]{H_v}$ [15].

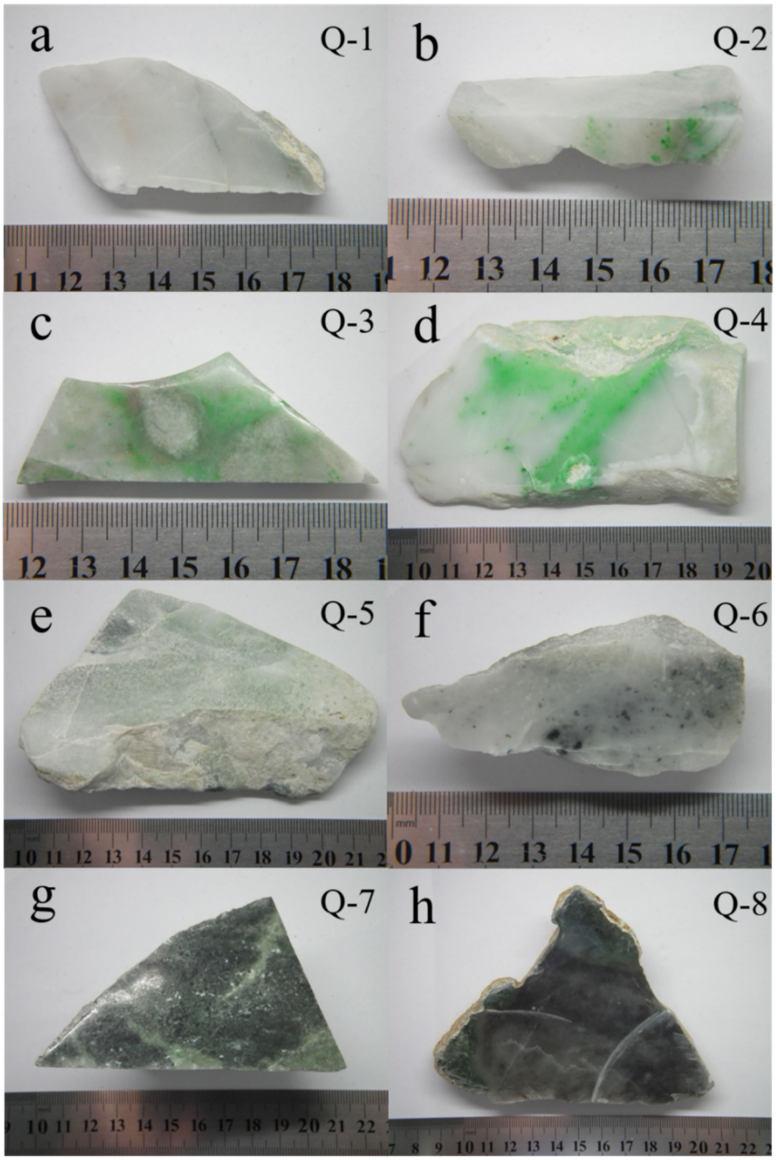

Figure 1. Selected samples of Philippines rock with different colors. (**a**) White sample Q-1; (**b**–**d**) green samples Q-2, Q-3, Q-4; (**e**) cyan-gray sample Q-5; (**f**) white sample with black spots Q-6, (**g**) dark green sample Q-7; (**h**) brown sample Q-8.

The samples were observed using a GI-MP22 gemological microscope using reflected light. The parts with characteristic colors were selected from each sample to prepare petrographic thin sections. This work was performed in the Yifu Building, China University of Geosciences, Beijing, China. The thin sections were observed and photographed using a BX51 polarized light microscope (PLM).

The chemical compositions of Philippines rock were determined in the Regional Geological Survey Institute of Hebei Province using a JEOLEMPA 8230 electron microprobe analyzer (EMPA). The instrument operating conditions included a spot size of 5 μm, an acceleration voltage of 15 kV and a beam current of 10 nA.

Fourier transform infrared (FTIR) spectra, Raman microprobe spectra, and UV-Vis spectra were acquired at the Experimental Teaching Center of Jewelry and Mineral Materials, China University of Geosciences, Beijing. The FTIR spectra for the eight polished samples were recorded in reflection mode using a Bruker Tensor 27 FTIR spectrometer. The analytical conditions used for measurement included a resolution of 4 cm^{-1}, a scan range of 100–1200 cm^{-1}, and a run time of 30 s per scan.

Based on assessment of the PLM observation, the EMPA data and the FTIR spectra, the petrographic thin sections corresponding to the different color samples were selected and measured using a Horiba Scientific Raman microprobe spectrometer. Analysis conditions included an excitation wavelength of 532 nm, a scan range of 100–1200 cm^{-1}, a resolution of 4 cm^{-1}, and a spot size of 5 μm; each spectrum was scanned three times for 5 s.

Each sample was polished and cut into square sections of 1×1 cm^2. The UV-Vis spectra were measured using a UV-3600 spectrophotometer (Shimadzu, Japan), and the main operating conditions were reflection mode, scan range of 300–800 nm, sampling interval of 5 s, and high-speed scan mode.

3. Results

3.1. Sample Appearance and Gemological Properties

The gemological properties of the samples are presented in Table 1. The white sample (Q-1) of delicate texture and smooth surfaces consisted mainly of white basal minerals. The green samples (Q-2–Q-4) consisted mainly of white basal minerals with green spots and green plaques. (Figure 2a). The green minerals were mostly euhedral–hypidiomorphic and the euhedral degree was relatively high (the cross-section was approximately hexagonal) (Figure 2b). There are a number of black spot minerals near the green mineral grains (Figure 2a). The cyan-gray sample (Q-5) consisted mainly of white and cyan-gray minerals (Figure 2c), and the luster was dimmer than the other samples. The white sample with black spots (Q-6) consisted mainly of white basal, black spots, and black plaque minerals (Figure 2d). The dark green sample (Q-7) consisted mainly of dark green to black-green and gray-green minerals (Figure 2e), and the grain size of the minerals was larger than those of the other samples. There are clear reflecting surfaces on the sample in the shape of "fly wings" as viewed under reflected light (Figure 2e), indicating that the cleavage of the basal minerals is well developed. The brown sample (Q-8) consisted mainly of white basal minerals, tan spots, and small black grains. There are some transparent "waterline" striations on the brown sample (Figure 2f).

Table 1. Gemological properties of the Philippines rock samples.

Sample	Color	Luster	RI	SG	H_M
Q-1	White	Vitreous luster	1.57	2.77	6.37
Q-2	Green	Vitreous luster	White part = 1.57 Green part > 1.78	2.69	6.40
Q-3	Green	Vitreous luster		2.74	6.22
Q-4	Green	Vitreous luster		2.76	6.15
Q-5	Cyan-gray	Greasy luster	1.63	2.83	6.11
Q-6	White with black spots	Vitreous luster	1.56	2.78	6.15
Q-7	Dark green	Vitreous luster	1.62	2.83	6.38
Q-8	Brown	Vitreous luster	1.58	2.73	6.23

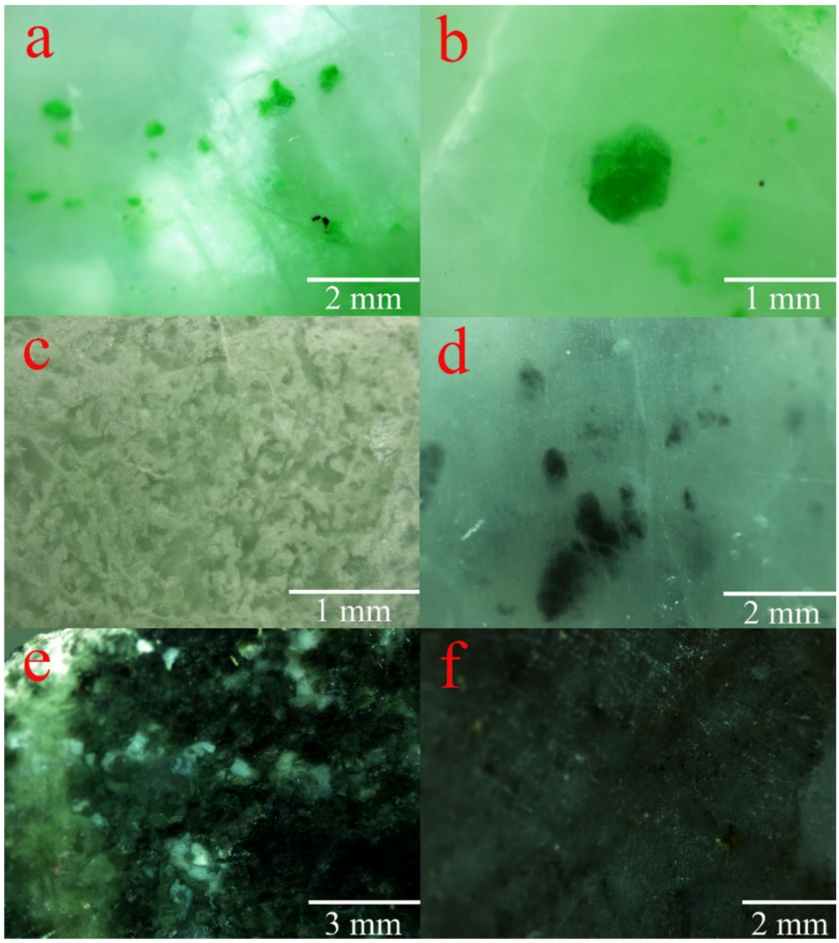

Figure 2. Mineral microstructure of the samples. (**a**) The green spots, green plaques, and black spots in Q-2; (**b**) the green mineral with high euhedral degree in Q-4; (**c**) the cyan-gray sample Q-5 consisting of white and cyan-gray minerals; (**d**) the spot and plaque minerals in the white sample with black spots Q-6; (**e**) image of the "fly wings" reflecting surfaces on the dark green sample Q-7; (**f**) the "waterline" striations on the brown sample Q-8.

3.2. Petrography

The observations of each mineral in the Philippines rock samples using PLM are shown in Figure 3. The analysis shows that the samples contain the major mineral plagioclase (Pl) with minor minerals diopside (Di), amphibole-supergroup mineral (Am), garnet-supergroup mineral (Gr), chromite (Chr), titanite (Ttn), zeolite (Zeo), prehnite (Prh), and zoisite (Zo). The characteristics of these minerals are as follows:

3.2.1. Plagioclase

Plagioclase is present in all samples in the forms of the matrix and phenocryst. It is the major mineral of the samples and also the dominant mineral at the magmatic stage. The plagioclase phenocryst is granular and short columnar in shape with a grain size about 0.01–2 mm. Some of the plagioclase phenocryst was fractured with disordered edges and was surrounded by small plagioclase grains, indicating that they had undergone dynamic metamorphism (Figure 3a).

3.2.2. Diopside

Diopside of different forms exists in the samples with the exception of the white and brown samples. Diopside in the cyan-gray sample and white sample with black spots is granular, short columnar and irregular with a grain size of about 100–500 μm (Figure 3b);

in the dark green sample, diopside is undergoing alteration to amphibole-supergroup mineral, and some of the diopside has altered completely (Figure 3c).

3.2.3. Amphibole-Supergroup Mineral

Amphibole-supergroup mineral only exists in the dark green sample, which is colorless and fibroid in nature. Some of the diopside alteration was incomplete in the vicinity of the amphibole-supergroup mineral (Figure 3c).

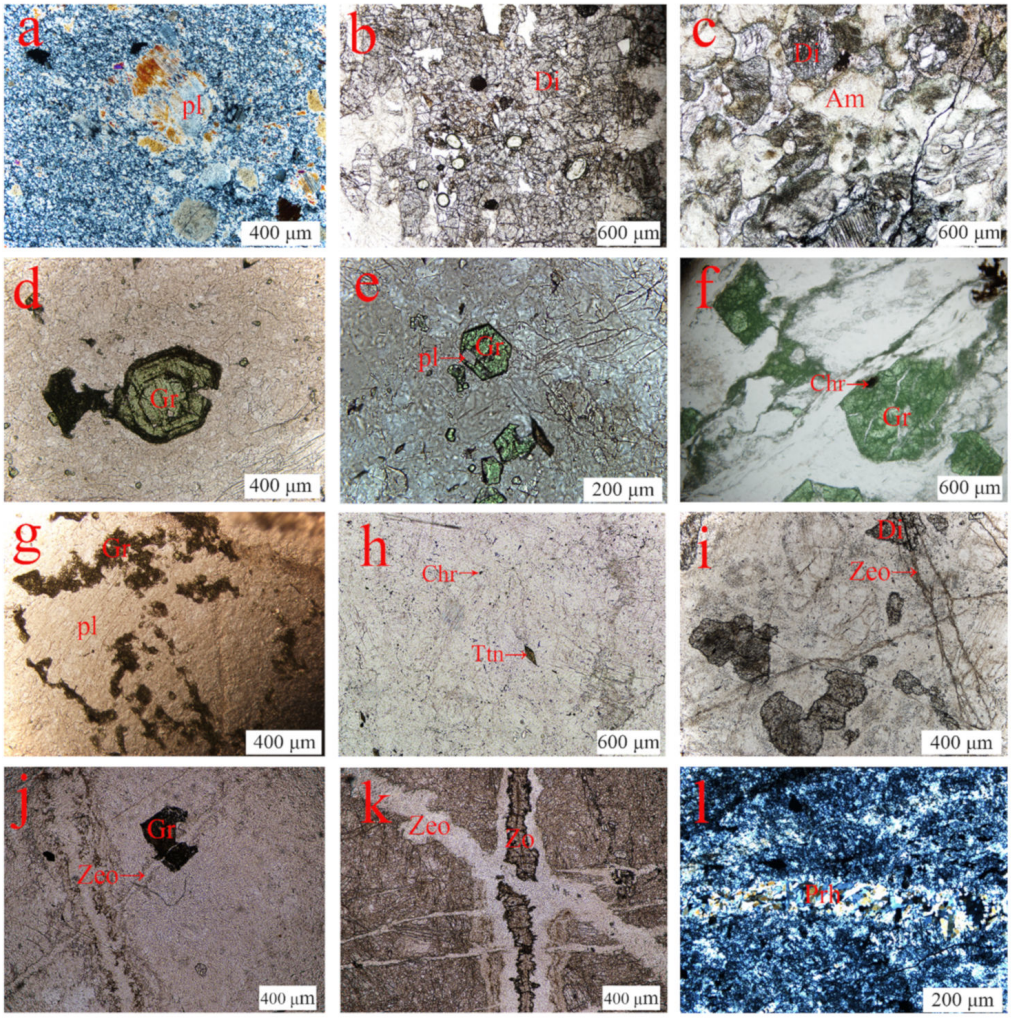

Figure 3. Mineral microstructural characteristics and paragenetic relationships of the samples under polarized light microscope (PLM). (**a**) The fractured plagioclase phenocryst surrounded by small plagioclase grains (Q-1); (**b**) the granular and short columnar diopside (Q-5); (**c**) the amphibole-supergroup mineral and the altered diopside (Q-7); (**d**) growth zones of the garnet-supergroup mineral (Q-4); (**e**) the fine-grained plagioclase as inclusions in the garnet-supergroup mineral (Q-4); (**f**) the chromite as inclusions in the garnet-supergroup mineral (Q-2); (**g**) the plagioclase phenocryst surrounded by small granular garnet-supergroup mineral (Q-3); (**h**) granular chromite and rhombic titanite (Q-8); (**i**) the zeolite vein cutting across the diopside (Q-6); (**j**) the zeolite vein cutting across the garnet-supergroup mineral (Q-3); (**k**) the zeolite vein cutting across the zoisite vein (Q-3); (**l**) the "mosaic"-like prehnite vein (Q-3). Pl, major mineral plagioclase; Di, minor minerals diopside; Am, amphibole-supergroup mineral; Gr, garnet-supergroup mineral; Chr, chromite; Ttn, titanite; Zeo, zeolite; Prh, prehnite; Zo, zoisite.

3.2.4. Garnet-Supergroup Mineral

The green minerals in the green samples are garnet-supergroup mineral with a grain size of about 0.01–1 mm. Some of garnet-supergroup mineral has a well-defined crystal shape and growth zones (Figure 3d). The granular plagioclase, chromite in the form of inclusions is present in the garnet-supergroup mineral (Figure 3e,f), and small garnet-supergroup mineral grains grow alongside the granular plagioclase (Figure 3g), indicating that the garnet-supergroup mineral was formed after the plagioclase and chromite and its growth conditions were related to the plagioclase.

3.2.5. Chromite and Titanite

The chromite and titanite may be readily identified in the brown rock sample. The chromite consists of black grains as well as inclusions in the garnet-supergroup mineral (Figure 3h,f). The titanite appears as rhombic and irregularly shaped granular crystals (Figure 3h). The chromite and titanite are both minerals of the magmatic stage.

3.2.6. Zeolite, Prehnite, and Zoisite

Zeolite, prehnite, and zoisite are present as vein-type structures. Some colorless vein-type zeolites cut across the diopside, garnet-supergroup mineral, and vein-type zoisite (Figure 3i–k). The prehnite vein has a special "mosaic" appearance (Figure 3l). The aforementioned minerals all formed in the late hydrothermal stage.

3.3. Mineral Chemistry

3.3.1. Plagioclase

The main chemical composition of plagioclase is $Na_{1-x}Ca_x[Al_{1+x}Si_{3-x}O_8]$. The plagioclase in the samples consists (wt.%) mainly of SiO_2 (42.96–44.60), Al_2O_3 (33.35–36.88), and CaO (18.23–19.76). Based on eight O atoms, the numbers of each cation and the end-member molecules of plagioclase were calculated (Table 2). The end members $An_{91.4–99}$ $Ab_{0.94–0.85}$ $Or_{0.01–0.91}$ were projected in the Or–Ab–An ternary system (Figure 4a,b) indicating that they belong to a range of anorthite ($Ab_{10–0}$ $An_{90–100}$) of the plagioclase isomorphous series [16].

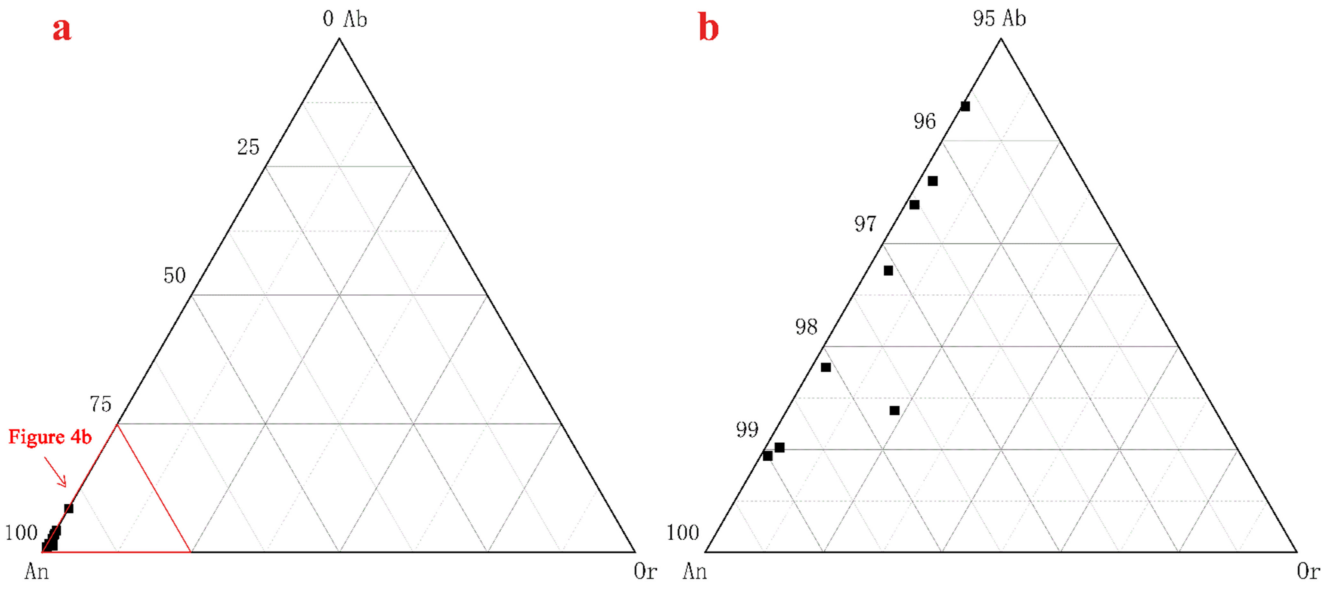

Figure 4. The Or–Ab–An ternary system showing that plagioclase in the samples is anorthite. (**a**) The end members $An_{91.4–99}$ $Ab_{0.94–0.85}$ $Or_{0.01–0.91}$ projected in the Or–Ab–An ternary system; (**b**) zoom-in of Figure 4a, showing that plagioclase in the samples is anorthite.

Table 2. Chemical compositions of the plagioclase (wt.%).

	Q-1	Q-2	Q-3	Q-4	Q-4	Q-5	Q-6	Q-7	Q-8
Na_2O	0.12	1.00	0.40	0.50	0.11	0.16	0.21	0.32	0.42
MgO	0.00	0.00	0.01	0.00	0.00	0.01	0.00	0.01	0.00
Al_2O_3	36.88	35.54	36.68	35.35	36.62	35.98	36.67	36.47	35.97
SiO_2	43.57	44.60	43.71	44.57	43.59	43.64	43.12	42.96	43.65
K_2O	0.02	0.00	0.01	0.01	0.01	0.15	0.02	0.03	0.02
CaO	19.76	18.23	19.25	18.72	19.67	19.28	19.52	19.33	19.11
TiO_2	0.01	0.00	0.00	0.00	0.00	0.00	0.01	0.00	0.01
Cr_2O_3	0.00	0.05	0.01	0.01	0.01	0.01	0.01	0.02	0.04
MnO	0.00	0.00	0.02	0.02	0.00	0.01	0.01	0.00	0.02
FeO	0.02	0.21	0.03	0.17	0.03	0.03	0.03	0.14	0.20
NiO	0.00	0.03	0.00	0.02	0.00	0.01	0.00	0.02	0.03
Total	100.38	99.67	100.12	99.36	100.04	99.28	99.60	99.30	99.47
Si	2.01	2.06	2.02	2.07	2.01	2.03	2.00	2.00	2.03
Ti	0.00	0.00	0.00	0.00	0.00	0.00	0.00	0.00	0.00
Al	2.00	1.94	1.99	1.93	1.99	1.97	2.01	2.00	1.97
Ca	0.98	0.90	0.95	0.93	0.97	0.96	0.97	0.97	0.95
Na	0.01	0.09	0.04	0.04	0.01	0.01	0.02	0.03	0.04
K	0.00	0.00	0.00	0.00	0.00	0.01	0.00	0.00	0.00
Fe	0.00	0.01	0.00	0.01	0.00	0.00	0.00	0.01	0.01
Mg	0.00	0.00	0.00	0.00	0.00	0.00	0.00	0.00	0.00
Cr	0.00	0.00	0.00	0.00	0.00	0.00	0.00	0.00	0.00
Mn	0.00	0.00	0.00	0.00	0.00	0.00	0.00	0.00	0.00
Ni	0.00	0.00	0.00	0.00	0.00	0.00	0.00	0.00	0.00
Total	5.00	5.00	5.00	4.98	4.98	4.98	5.00	5.01	5.00
Or	0.12	0.02	0.08	0.03	0.06	0.91	0.12	0.18	0.12
Ab	1.02	8.58	3.38	4.34	0.94	1.38	1.80	2.74	3.61
An	98.87	91.40	96.54	95.63	99.00	97.71	98.08	97.08	96.27

3.3.2. Garnet-Supergroup Mineral

The main chemical composition of garnet-supergroup mineral is $A_3B_2[SiO_4]_3$. The garnet-supergroup mineral in the green samples consists (wt.%) mainly of SiO_2 (37.56–38.32), CaO (33.62–34.90), Cr_2O_3 (12.13–15.64), and Al_2O_3 (6.70–10.91). The numbers of each cation and the end-member molecules of garnet-supergroup mineral were calculated (Table 3). The end members of garnet-supergroup mineral range from $Uvt_{40.51}$ $Grs_{46.68}$ $Adr_{11.69}$ $Prp_{1.12}$ $Sps_{0.01}$ to $Uvt_{50.95}$ $Grs_{41.65}$ $Adr_{5.56}$ $Prp_{1.80}$ $Sps_{0.24}$. The main mineral component of the garnet-supergroup mineral in the green samples is uvarovite-grossular-andradite solid-solution of the Ca-garnet series with high Cr content, among which the uvarovite-grossular is predominant [17].

3.3.3. Diopside

The main chemical composition of diopside is $CaMg[Si_2O_6]$.The diopside in the samples consists (wt.%) of SiO_2 (52.44–55.63), CaO (22.55–25.65), and MgO (15.77–18.21). The numbers of cations in the diopside are listed in Table 4.

Table 3. Chemical compositions of the garnet-supergroup mineral (wt.%).

Samples	Q-2	Q-2	Q-3	Q-3	Q-3	Q-4	Q-4	Q-4
Na_2O	0.02	0.07	0.01	0.06	0.01	0.01	0.06	0.00
MgO	0.36	0.25	0.55	0.38	0.33	0.40	0.42	0.36
Al_2O_3	9.19	9.27	6.70	8.87	10.51	10.21	10.10	10.91
SiO_2	37.80	38.32	37.82	37.56	37.78	37.75	37.90	38.10
K_2O	0.00	0.02	0.00	0.00	0.00	0.02	0.02	0.00
CaO	34.49	33.62	34.90	33.84	34.43	34.58	34.14	33.95
TiO_2	2.40	0.40	2.08	0.66	0.93	1.01	0.61	0.91
Cr_2O_3	12.83	14.02	15.64	14.36	12.13	12.93	13.81	12.27
MnO	0.09	0.07	0.02	0.10	0.00	0.05	0.06	0.00
FeO	2.68	3.17	1.59	3.18	3.26	2.52	2.78	2.69
NiO	0.00	0.01	0.05	0.00	0.00	0.01	0.02	0.01
Total	99.86	99.21	99.35	99.01	99.38	99.50	99.93	99.20
Si	3.01	3.07	3.05	3.02	3.00	3.00	2.99	2.99
Ti	0.14	0.02	0.13	0.04	0.06	0.06	0.04	0.04
Al	0.86	0.87	0.64	0.84	0.99	0.96	0.95	0.95
Cr	0.81	0.89	1.00	0.91	0.76	0.81	0.87	0.87
Fe^{3+}	0.18	0.21	0.11	0.21	0.22	0.17	0.19	0.18
Fe^{2+}	0.00	0.00	0.00	0.00	0.00	0.00	0.00	0.00
Mn	0.01	0.00	0.00	0.01	0.00	0.00	0.00	0.00
Mg	0.04	0.03	0.07	0.05	0.04	0.05	0.05	0.05
Ca	2.94	2.88	3.01	2.91	2.93	2.95	2.91	2.91
Na	0.00	0.01	0.00	0.01	0.00	0.00	0.01	0.01
Total	8.00	8.00	8.00	8.00	8.00	8.00	8.00	8.00
Grs	46.37	39.76	41.65	38.81	46.68	46.68	42.35	42.64
Adr	9.58	11.58	5.56	11.46	11.69	8.98	9.99	9.67
Uvt	42.64	47.63	50.95	48.19	40.51	42.88	46.11	46.13
Prp	1.21	0.86	1.80	1.29	1.12	1.34	1.41	1.41
Alm	0.00	0.00	0.00	0.00	0.00	0.00	0.00	0.00
Sps	0.21	0.17	0.03	0.24	0.01	0.12	0.15	0.15

Grs-grossular; Adr-andradite; Uvt-uvarovite; Prp-pyrope; Alm-almandine; Sps-spessartine.

Table 4. Chemical compositions of the diopside (wt.%).

Samples	Q-4	Q-5	Q-5	Q-6	Q-6	Q-7
Na_2O	0.05	0.02	0.03	0.05	0.17	0.21
MgO	17.06	17.93	18.21	18.14	15.89	15.77
Al_2O_3	0.68	2.14	1.44	1.51	1.13	2.90
SiO_2	55.63	53.69	54.07	54.00	54.40	52.44
K_2O	0.00	0.02	0.00	0.03	0.01	0.00
CaO	25.44	25.41	25.33	25.65	23.53	22.55
TiO_2	0.10	0.16	0.23	0.26	0.10	0.22
Cr_2O_3	0.02	0.01	0.03	0.03	0.08	0.32
MnO	0.10	0.00	0.02	0.00	0.15	0.16
FeO	0.59	0.76	0.53	0.61	4.67	4.67
NiO	0.01	0.01	0.00	0.00	0.00	0.04
Total	99.69	100.16	99.88	100.27	100.13	99.26
Si	2.02	1.93	1.95	1.94	1.99	1.94
Ti	0.00	0.00	0.01	0.01	0.00	0.01
Al	0.03	0.09	0.06	0.06	0.05	0.13
Cr	0.00	0.00	0.00	0.00	0.00	0.01
Fe^{3+}	0.00	0.02	0.02	0.02	0.00	0.00
Fe^{2+}	0.03	0.00	0.00	0.00	0.14	0.14
Mn	0.00	0.00	0.00	0.00	0.01	0.01
Ni	0.00	0.00	0.00	0.00	0.00	0.00
Mg	0.92	0.96	0.98	0.97	0.87	0.87
Ca	0.99	0.98	0.98	0.99	0.92	0.89
Na	0.00	0.00	0.00	0.00	0.01	0.02
K	0.00	0.00	0.00	0.00	0.00	0.000
Total	3.99	3.98	4.00	3.99	3.99	4.02

3.3.4. Amphibole-Supergroup Mineral

The main chemical composition of amphibole-supergroup mineral is $A_{0–1}B_2C_5[T_4O_{11}]_2(OH,F,Cl)_2$. The amphibole-supergroup mineral in the dark green samples consists (wt.%) mainly of SiO_2 (53.95–55.91), CaO (12.59–13.86), MgO (20.92–23.69), Al_2O_3 (2.93–3.94), and

FeO (2.02–3.59). The numbers and site occupancy of each cation, based on 23 O atoms, were calculated, and are given in Table 5. It is shown that the amphibole-supergroup mineral is a member of the calcic group with $(Na + Ca)_B \geq 1.5$ and $Na_B < 0.5$ ($(Ca + Na)_B \geq 1.73$, $Na_B < 0.07$). At the same time, it can be determined that the dark green to black-green minerals with $Mg/(Mg + Fe^{2+}) \geq 0.9$ and $Si^{4+} > 7.5$ ($Mg/(Mg + Fe^{2+}) \geq 0.94$, $Si^{4+} > 7.52$) in Q-7 is tremolite [18].

Table 5. Chemical compositions of the amphibole-supergroup mineral (wt.%).

Samples	Q-7	Q-7	Q-7	Q-7
Na_2O	0.29	0.14	0.25	0.21
MgO	21.72	21.98	20.92	23.69
Al_2O_3	3.03	3.10	3.94	2.93
SiO_2	55.33	55.91	54.99	53.95
K_2O	0.01	0.08	0.11	0.09
CaO	13.86	13.53	12.59	12.97
TiO_2	0.17	0.06	0.02	0.02
Cr_2O_3	0.31	0.01	0.03	0.02
MnO	0.04	0.22	0.26	0.04
FeO	2.35	2.02	3.59	2.87
NiO	0.02	0.01	0.00	0.00
Total	97.12	97.05	96.70	96.78
Si	7.68	7.71	7.63	7.52
Al^{IV}	0.32	0.29	0.37	0.48
∑T	8.00	8.00	8.00	8.00
Al^{VI}	0.18	0.22	0.28	0.00
Ti	0.02	0.01	0.00	0.00
Fe^{3+}	0.00	0.01	0.13	0.00
Cr	0.03	0.00	0.00	0.00
Mg	4.49	4.52	4.33	4.92
Ni	0.00	0.00	0.00	0.00
Fe^{2+}	0.27	0.22	0.26	0.07
Mn	0.01	0.03	0.00	0.00
∑C	5.00	5.01	5.00	4.99
Fe	0.00	0.00	0.03	0.26
Mn	0.00	0.00	0.03	0.01
Ca	2.00	2.00	1.87	1.73
Na	0.00	0.00	0.07	0.00
∑B	2.00	2.00	2.00	2.00
Ca	0.06	0.00	0.00	0.20
Na	0.08	0.04	0.00	0.06
K	0.00	0.01	0.02	0.02
∑A	0.14	0.05	0.02	0.28
$Mg^{2+}/(Mg^{2+} + Fe^{2+})$	0.94	0.95	0.94	0.99

3.3.5. Chromite, Titanite, Thomsonite-Ca, Prehnite, Zoisite, and Chlorite

The EPMA data for chromite, titanite, thomsonite-Ca, prehnite, zoisite, and chlorite in the samples are presented in Table A1.

3.4. Spectroscopy

3.4.1. FTIR Spectra

The FTIR reflectance spectra for all samples are quite similar (Figure 5a), and the reflection peaks are in the 400–1200 cm^{-1} frequency range (Figure 5b). The band at 426 cm^{-1} is due to the Si–O–Si deformation, and the bands at 468, 484, and 539 cm^{-1} are attributed to the O–Si–O bending and the Ca–O stretching modes. The bands at 568, 585, 602, and 627 cm^{-1} are caused by the O–Si(Al)–O bending mode. The bands at 726 and 757 cm^{-1} are ascribed to the Si–Si(Al) and the Si–Si stretching modes, respectively. The bands at 931 and 945, which are the two strongest bands in the spectrum, and the bands

at 910 and 1022 cm^{-1} are caused by the Si(Al)–O stretching mode. The bands at 1103 and 1143 cm^{-1} are caused by the Si–O stretching mode [19,20]. These bands are related to the structure of anorthite, indicating that anorthite is the main mineral of the Philippines rock samples. There are small deviations in the Raman bands for the different samples. The two strongest bands for the green samples Q-2 and Q-3 are 923 and 925 cm^{-1} (Figure 5c), which are related to the [SiO_4] stretching mode in garnet-supergroup mineral and the Si(Al)–O stretching mode in anorthite. Q-5 also shows bands at 823 and 844 cm^{-1} caused by the [SiO_4] stretching mode [21,22]. There is no garnet-supergroup mineral in Dushan jade. The bands at 823, 844, 923, and 925 cm^{-1} may be used to differentiate the green Philippines rock from the green Dushan jade.

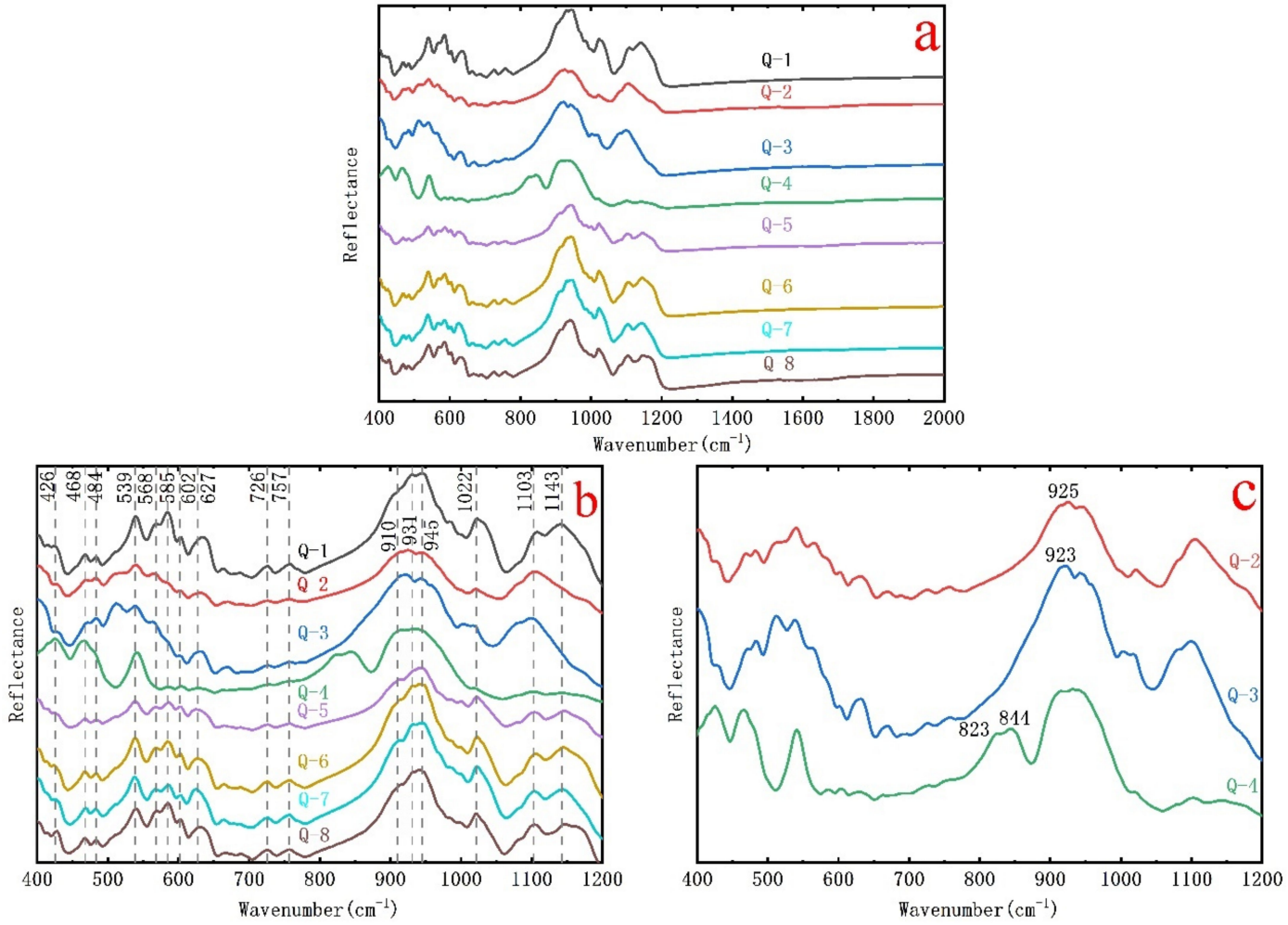

Figure 5. FTIR spectra of the samples. (**a**) FTIR spectra for all samples for the 400–2000 cm^{-1} frequency range; (**b**) FTIR spectra for all samples for the 400–1200 cm^{-1} frequency range; (**c**) FTIR spectra for the green samples for the 400–1200 cm^{-1} frequency range.

3.4.2. Raman Microprobe Spectroscopy

Based on the results for PLM, the FTIR spectra, and EMPA, Raman microprobe studies were undertaken based on measurement of the petrographic thin sections at selected regions of interest. Anorthite, the main mineral in Philippines rock, was detected in all samples (Figure 6a). The strongest band at 505 cm^{-1} corresponds to the bending vibration of the bridging O. Ca^{2+} occupies the central M position in anorthite, and to maintain the electrochemical balance, Al enters the silicate framework, which leads to the band at 505 cm^{-1} associated with the bridging O further splitting into 487 and 556 cm^{-1}. The bands at 147–401 cm^{-1} are assigned to the M–O lattice modes. The band at 763 cm^{-1} may

be due to the symmetrical stretch mode of Al^{IV}–O_{nb} (non-bridging O) and the bands at 913, 956, and 983 cm^{-1} are caused by the antisymmetric stretching mode of Al–O–Si [23,24]. The Raman microprobe spectra for diopside, uvarovite, chromite, thomsonite-Ca, prehnite, tremolite, and titanite were also analyzed (Figure 6b–h), and the assignments of the Raman shifts are listed in Table 6.

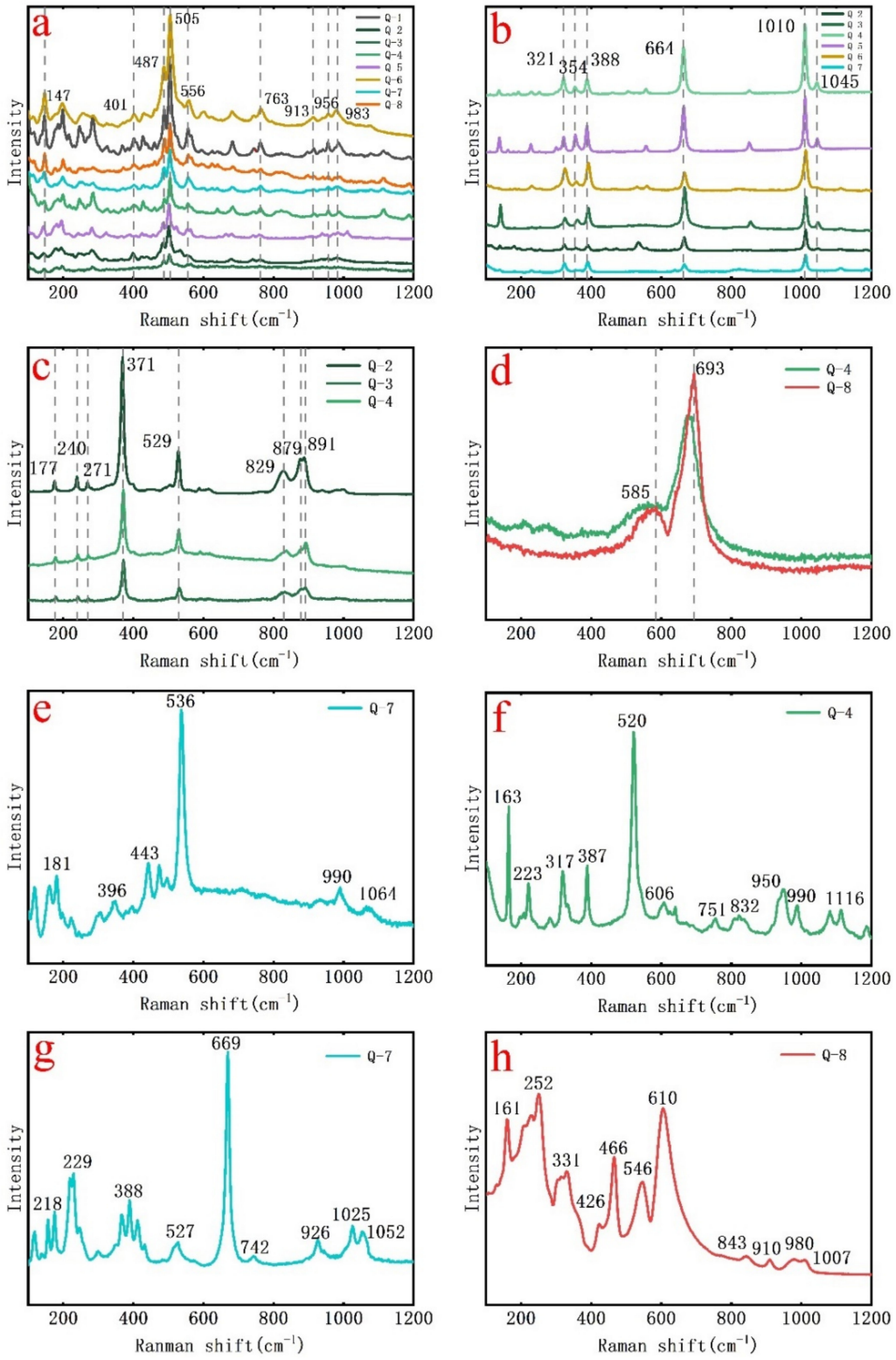

Figure 6. The Raman microprobe spectra for different minerals in the rock samples. (**a**) Anorthite; (**b**) diopside; (**c**) uvarovite; (**d**) chromite; (**e**) thomsonite-Ca; (**f**) prehnite; (**g**) tremolite; (**h**) titanite.

Table 6. The assignments of the different minerals (after Raman microprobe measurement).

Minerals	Raman Shift, cm^{-1}	Assignment	Reference
Diopside	321, 354, 388	Mg–O	[25]
	664	δ(Si–O–Si)	
	1010	V_s(Si–O)	
	1045	V_{as}(Si–O)	
Uvarovite	177	Ca–M	[22,26]
	240, 271	$[SiO_4]_R$	
	371	$[SiO_4]_T$	
	529	δ(Si–O)	
	829, 879	V_{as}(Si–O)	
	891	V_s(Si–O)	
Chromite	585,693	$V_s(^MBO^6)$	[27,28]
Thomsonite-Ca	117, 159, 181, 197, 222, 348, 307, 396	Ca–M	[29,30]
	443, 473, 496, 536	δ(O–T–O)	
	990, 1064	V_{as}(T–O–T)	
Prehnite	163, 223, 286, 317, 387	M–O	[31,32]
	520	V_s(T–O–T)	
	606, 641, 751, 832	δ(O–T–O)	
	950, 990, 1080, 1116, 1187	Stretching and bending of Si–O and T–O–T	
Tremolite	118, 155, 175, 218, 229, 367, 388, 411	Ca–O Mg–O	[33–35]
	527	δ(Si–O)	
	669, 742	V_s(Si–O–Si)	
	926, 1025, 1052	V_s(Si–O)	
Titanite	161, 230, 252, 317, 331	Ca–O Ti–O Si–O	[36–38]
	426, 466	δ(Si–O)	
	546, 610	V(Ti–O)	
	843, 910, 980, 1007	V(Si–O)	

v, stretching; δ, deformation; $_s$,symmetric; $_{as}$, antisymmetric; T can be Al/Si, Al–O–Al linking is forbidden. $[SiO_4]_T$-translational mode of $[SiO_4]$; $[SiO_4]_R$-rotational mode of $[SiO_4]$.

3.4.3. UV-Visible Spectra

The minerals responsible for color in the Philippines rock samples are uvarovite, diopside, and tremolite. According to the EMPA data, the main chromogenic cations are Cr^{3+}, Fe^{2+}, and Fe^{3+}, and the color of the Philippines rock samples is intense. To further explore the origin of color generation, the UV-Vis spectra of samples were recorded on the same basis as for EMPA (Figure 7a–e). The analysis show that the colors are attributed mainly to electron transitions and charge transfer. The specific color geneses are listed in Table 7.

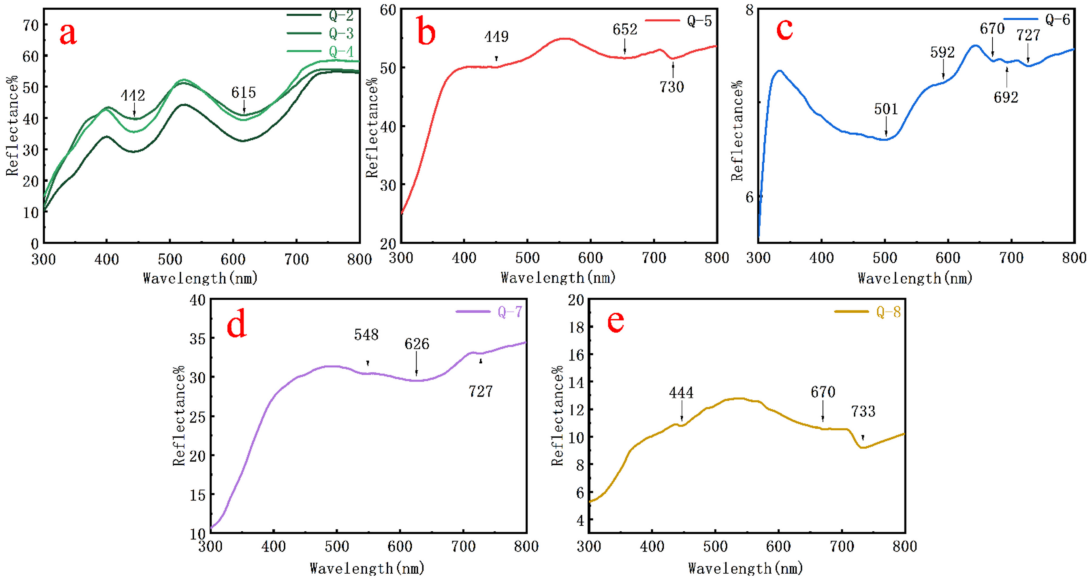

Figure 7. UV-Vis spectra for the Philippines rock samples. (**a**) UV-Vis spectra for the green samples Q-2–Q-4; (**b**) UV-Vis spectra for the cyan-gray sample Q–5; (**c**) UV-Vis spectra for the white sample with black spots Q–6; (**d**) UV-Vis spectra for the dark green sample Q–7; (**e**) UV-Vis spectra for the brown sample Q–8.

Table 7. The origins of color for the Philippines rock samples.

Samples	Color	Reflection Peak	Color Origin	Reference
Q-2 Q-3 Q-4	Green	442 nm 615 nm	Cr^{3+}:$^4A_{2g}(F) \rightarrow {}^4T_{1g}(F)$ Cr^{3+}:$^4A_{2g}(F) \rightarrow {}^4T_{2g}(F)$	[39]
Q-5	Cyan-gray	449 nm 652 nm 730 nm	$O^{2-} \rightarrow Fe^{3+}$ Cr^{3+}:$^4A_{2g} \rightarrow {}^4T_{2g}$ Fe^{2+}:$^5T_2(D) \rightarrow {}^3T_2(H)$	[40–44]
Q-6	White with black spots	548 nm 626 nm 727 nm	Fe^{2+}:$^5T_2(D) \rightarrow {}^3T_2(G)$ Cr^{3+}:$^4A_{2g} \rightarrow {}^2T_{1g}$ Fe^{2+}:$^5T_2(D) \rightarrow {}^3T_2(H)$	[40,43,44]
Q-7	Dark green	444 nm 670 nm 733 nm	Fe^{3+}:$^6A_1 \rightarrow 4A_1{}^4E(G)$ Cr^{3+}:$^4A_{2g} \rightarrow {}^2T_{1g}$ Fe^{2+}:$^5T_2(D) \rightarrow {}^3T_2(H)$	[43,44]
Q-8	Brown	501 nm 592 nm 670 nm 727 nm	Fe^{2+}:$^5T_2(D) \rightarrow {}^3T_2(bF)$ $Fe^{2+} \rightarrow Fe^{3+}$ Cr^{3+}:$^4A_{2g} \rightarrow {}^2T_{1g}$ Fe^{2+}:$^5T_2(D) \rightarrow {}^3T_2(H)$	[40,42,44,45]

4. Discussion

4.1. Origin of the Green Color in the Rock Samples

The most precious Philippines rock sample is the green variety. The green color of the samples originates from the presence of uvarovite. Uvarovite is the rarest of the garnet group and often exists as a solid-solution with grossular and andradite [46]. The Ca-garnets with uvarovite as the dominant end member are usually found in skarn, serpentinite, and metamorphosed limestones, and often in association with chromite [47,48]. The uvarovite can be a replacement product of relic chromite [49,50].

Mogessie and Rammlmair found that the uvarovite was formed at the edge of chromite in the form of inclusions in grossular-andradite, which was clearly zoned (the inner zone is uvarovite with high Cr content while the outer zone is grossular-andradite with a sharp decrease in Cr content) [51]. The garnet-supergroup mineral not including dissolved chromite is all in the form of unzoned grossular-andradite solid-solution. The reaction of uvarovite is as follows:

chromite + grossular-andradite = uvarovite + grossular-andradite [51].

Liu believes that the origin of uvarovite in Philippines rock is the same as the above [12]. In this study, it was found that all the garnet-supergroup minerals are in the form of the uvarovite-grossular-andradite solid-solution (Table 3), and the uvarovite including chromite is not zoned, indicating that the uvarovite in Philippines rock could not form by the above reaction. Pal and Das found that the uvarovite in association with chromite could be formed by cooling and crystallization of the hydrothermal solution, and that the Cr was derived from the dissolution or metamorphism of chromite, but the source of Ca was uncertain [52]. In the present study, it was found that the anorthite was surrounded by uvarovite (Figure 3g), indicating that it had provided material conditions for the formation of uvarovite. The EMPA confirmed that Ca and Al were present (Table 2). Finally, it was determined that the uvarovite in Philippines rock was formed by hydrothermal solution. The dissolved chromite released Cr and Fe while anorthite released Ca and Al into the hydrothermal solution, which provided material conditions for the formation of uvarovite (uvarovite-grossular-andradite solid-solution).

4.2. The Paragenetic Relationship

The anorthite, abundant in all colored samples, is the main mineral of Philippines rock. The residual anorthite phenocryst was surrounded by the fine-grained anorthite of uniform size (Figure 3a). The boundary between the fine-grained anorthite and the residual phenocryst is highly irregular, and the optical orientations are different, showing that the

anorthite, which formed in the magmatic stage, underwent metamorphism, which resulted in fragmentation, refinement, and recrystallization under stress [6]. The diopside, the most important minor mineral in the samples, anorthite, chromite, and titanite belong to the magmatic stage. The fibrous tremolite, which was only present in the dark green sample, underwent alteration from the diopside and retains the original outline of the diopside (Figure 3c).

Uvarovite exists only in the green samples, and the uvarovite, which has grown and includes the fine-grained anorthite (Figure 3e), indicates that it was formed after dynamic metamorphism. Although the importance of a hydrothermal solution for uvarovite formation has been discussed, the uvarovite cut by the veinlike thomsonite-Ca (Figure 3j) indicates that there were multi-stages associated with the hydrothermal solution after metamorphism, and the formation of uvarovite and thomsonite-Ca did not belong to the same stage.

The mineral paragenetic sequence was determined: anorthite phenocryst, diopside, chromite, and titanite were formed in the magmatic stage; in the metamorphic stage, anorthite phenocryst was fractured and recrystallized; and the early fluid intrusion altered diopside into tremolite and formed uvarovite-grossular-andradite solid-solution around the anorthite and chromite; the late hydrothermal solution filled in fractures and formed prehnite, thomsonite-Ca, and zoisite. A small amount of chlorite detected by EMPA may be derived from the chloritization of tremolite or diopside. The mineral assemblages and structural characteristics of Philippines rock are given in Table 8.

Table 8. The mineral assemblages and structural characteristics of Philippines rock.

Color	Mineral Assemblages	Structural Characteristics
White	Anorthite	Porphyroblastic texture
Green	Anorthite, uvarovite, thomsonite-Ca, diopside, zoisite, prehnite, chromite	Porphyroblastic texture and fine-grained granoblastic texture
Cyan-gray	Anorthite, diopside	Granoblastic texture and inequigranoblastic texture
White with black spots	Anorthite, diopside, thomsonite-Ca	Porphyroblastic texture and granoblastic texture
Dark green	Diopside, tremolite, anorthite, chlorite, thomsonite-Ca	Granoblastic texture
Brown	Anorthite, titanite, chromite	Granoblastic texture

4.3. Comparison with Dushan Jade

In the gemstone market in China, the material in question is called Philippines "Dushan jade". Therefore, a comparison of various properties of Dushan jade and Philippines rock has been undertaken (Table 9). In support of this, a number of studies on the gemology, mineralogy, and petrology of Dushan jade have been reported [5–10]. Authentic Dushan jade is composed predominantly of plagioclase (anorthite) and zoisite, with minor amounts of chrome mica, biotite, diopside, amphibole-supergroup mineral, titanite, rutile, epidote, actinolite, and tourmaline, which is zoisitized anorthosite [6–9]. In contrast, the main mineral in Philippines rock is anorthite, not zoisite, with minor amounts of diopside, tremolite, uvarovite, titanite, chromite, zoisite, prehnite, thomsonite-Ca, and chlorite. Given that both types of material contain a large amount of anorthite, the IR spectra of the two types of material are similar with most peaks being caused by anorthite (Figure 5b).

Dushan jade has a variety of colors, including white, green, purple, yellow, pink, and black, which is quite different from Philippines rock. The two types of material are only similar with respect to the appearance of the green samples, both of which have a granular texture, a massive structure, and a vitreous luster. The main color causing minerals of green Philippines rock are uvarovite, while the green of Dushan jade originates from the chrome mica, epidote, diopside; that is, garnet-supergroup mineral is absent in Dushan jade. In the infrared spectra, the bands at 823, 844, 923, and 925 cm^{-1} in this work, which are related to

garnet-supergroup mineral, do not appear in green Dushan jade (Table A2). Furthermore, the Raman microprobe spectra for the green minerals in Philippines rock and Dushan jade are completely different. The bands in the former are assigned to the uvarovite, while the bands in the latter are associated with the chrome mica, epidote, and diopside.

Table 9. Comparison of properties of Dushan jade and Philippines rock.

	Dushan Jade [53]	**Philippines Rock**
Mineral Composition	Composed mainly of plagioclase (anorthite) and zoisite, with minor amounts of chrome mica, biotite, diopside, amphibole-supergroup mineral, titanite, rutile, epidote, actinolite, tourmaline	Composed mainly of anorthite, with minor amounts of diopside, tremolite, uvarovite, titanite, chromite, zoisite, prehnite, thomsonite-Ca, and chlorite
Texture	Granular texture	Granular texture
Structure	Massive structure	Massive structure
Color	White, green, blue-green, purple, yellow, black, pink.	White, green, cyan-gray, white with black spots, dark green, brown
Luster	Vitreous luster	Vitreous luster, greasy luster
Transparency	Sub-translucent, semi- translucent	Sub-translucent, non-transparent
RI	RI = 1.56–1.70	RI = 1.56–1.63, green part > 1.78
Fluorescence	Inert to weak, bluish-white, brown-yellow, brown-red	Inert under LW, purple-red under SW
SG	2.70–3.09	2.69–2.83
Mohs Hardness	6–7	6.11–6.40
Rock Type	Zoisitized anorthosite	Tremolitized diopside anorthosite

The rock type of Dushan jade belongs to zoisitized anorthosite. Anorthite, the major mineral of Philippines rock, belongs to the plagioclase isomorphous series. Diopside is the minor mineral with the highest content in Philippines rock and was altered by tremolitization. According to the nomenclature for metamorphic rocks [54], the rock type of Philippines rock belongs to "tremolitized diopside anorthosite."

5. Conclusions

In this research, we conducted a systematic study on the gemology, mineralogy, and spectroscopy of Philippines rock with the aim of ascertaining the rock type and to differentiate the Philippines rock from Dushan jade and hence be able to provide correct guidance to consumers.

Philippines rock is composed predominantly of anorthite with minor amounts of diopside, tremolite, uvarovite, titanite, chromite, zoisite, prehnite, thomsonite-Ca, and chlorite, among which the uvarovite, diopside, and tremolite are the main color causing minerals. The color is caused by the electronic transition of Cr^{3+}, Fe^{2+}, Fe^{3+}, and charge transfer between the ions. The mineral paragenetic sequence of Philippines rock can be divided into the magmatic stage, the metamorphic stage, and the late hydrothermal stage.

Philippines rock and Dushan jade are completely different types of rock, being only similar in appearance for the green forms of the material. Although both types are mainly composed of anorthite, the color causing minerals of Philippines rock and Dushan jade differ. The former is due to the presence of uvarovite, while the latter are caused by the presence of chrome mica, epidote, diopside. The FTIR and Raman microprobe spectra can be performed to differentiate the Philippines rock from Dushan jade. According to the nomenclature of metamorphic rocks, Philippines rock is termed "tremolitized diopside anorthosite."

Author Contributions: Conceptualization, X.Y.; Methodology, X.Y. and F.B.; Validation, X.Y., F.B., M.L., and H.S.; Formal analysis, X.Y.; Investigation, X.Y., F.B., M.L., and H.S.; Resources, X.Y., F.B., M.L., and H.S.; Data curation M.L. and H.S.; Writing—original draft preparation, X.Y.; Writing—review and editing, F.B.; Visualization, X.Y.; Supervision, F.B.; Project administration, F.B. All authors have read and agreed to the published version of the manuscript.

Funding: This research received no external funding.

Data Availability Statement: Not applicable.

Acknowledgments: Thanks to the School of Gemmology, China University of Geoscience, Beijing, and the Regional Geological Survey Institute of Hebei Province.

Conflicts of Interest: The authors declare no conflict of interest.

Appendix A

Table A1. Chemical compositions of zoisite, prehnite, chromite, thomsonite-Ca, titanite, and chlorite in the rock samples.

Samples	Q-2	Q-3	Q-4	Q-2	Q-3	Q-4	Q-4	Q-8	Q-8	Q-3	Q-4	Q-8	Q-8	Q-7
Minerals		**Zoisite**			**Prehnite**			**Chromite**			**Thomsonite-Ca**		**Titanite**	**Chlorite**
Na_2O	0.10	0.41	0.01	0.10	0.15	0.09	0.11	0.16	0.06	3.62	3.40	0.02	0.01	0.02
MgO	0.13	0.11	0.01	0.11	0.03	0.06	0.99	2.70	2.07	0.00	0.00	0.03	0.03	32.39
Al_2O_3	32.98	32.63	32.73	23.84	23.42	23.67	17.88	12.47	4.09	31.54	30.69	2.29	1.24	12.62
SiO_2	39.84	39.74	39.90	43.79	43.76	43.18	1.06	1.17	0.22	38.75	38.22	31.11	30.44	38.53
K_2O	0.03	0.10	0.09	0.03	0.00	0.01	0.00	0.03	0.00	0.02	0.02	0.02	0.01	0.03
CaO	23.42	22.91	23.95	26.34	26.58	27.29	0.54	0.74	0.85	12.99	12.69	28.33	27.79	0.29
TiO_2	0.01	0.01	0.01	0.32	0.91	0.94	0.17	0.01	1.48	0.02	0.00	35.83	37.19	0.05
C_r2O_3	0.01	0.02	0.00	0.01	0.04	0.09	46.76	52.33	60.86	0.04	0.03	0.01	0.05	0.09
MnO	0.05	0.09	0.28	0.04	0.00	0.06	1.96	1.32	0.74	0.05	0.05	0.01	0.04	0.03
FeO	1.21	1.24	0.13	0.62	0.16	0.18	29.69	28.96	29.18	0.03	0.02	0.21	0.39	0.63
NiO	0.00	0.00	0.00	0.00	0.00	0.00	0.00	0.00	0.02	0.04	0.00	0.00	0.01	0.00
Total	97.77	97.25	97.11	95.20	95.05	95.57	99.15	99.89	99.55	87.09	85.10	97.86	97.20	84.68

Q-1 (white rock sample) is composed totally of anorthite.

Table A2. Infrared absorption bands for the representative Dushan jade [55].

Color	Wavenumber, cm^{-1}																				
Green	280–400	447	474	488	518		578		625	660	700	720	758	777	866	910	950			1120	
Grey-green	310–407		474	488		542	580	603	624	667	700	730	760	770			940	1015	1095		1140
Luminous Green	310–410		475	488		542	580	605	624	667	700	730	760				930	1018	1080		1140
Brown-green	310–408		471	485	515	540	578	602	623	663	698	728	758				927	1015	1090		1140

References

1. GB/T 16552–2017. *Gems-Nomenclature*; Standardization Administration of China Press: Beijing, China, 2017. (In Chinese)
2. Wang, Y.Y.; Gan, F.X.; Zhao, H.X. Inclusions of black-green serpentine jade determined by Raman spectroscopy. *Vib. Spectrosc.* **2013**, *66*, 19–23. [CrossRef]
3. Wang, R. Progress review of the scientific study of Chinese ancient jade. *Archaeometry.* **2011**, *53*, 674–692. [CrossRef]
4. Zhao, H.X.; Li, Q.H.; Liu, S. Investigation of some Chinese jade artifacts (5000 BC to 771 BC) by confocal laser micro-Ranmen spectroscopy and other techniques. *J. Raman Spectrosc.* **2016**, *47*, 545–552. [CrossRef]
5. Liao, Z.T.; Zhao, J.; Zhou, Z.Y. On the Tectonic Setting and Origin of Dushan Jade Deposit in Nanyang. *J. Tongji Univ.* **2000**, *28*, 702–707, (In Chinese with English abstract).
6. Xiao, Q.Y.; Cai, K.Q.; Jiang, F.J. Tentative Discussion on the Mineral Cataclasis Jade-forming Process of Dushan Jade in Nanyang City, Henan Province. *Acta Geosci. Sin.* **2009**, *30*, 607–615, (In Chinese with English abstract).
7. Luo, Y.; Li, D.; Jiang, Y.H.; Li, N.B.; Yan, S.; Shan, Q. Geochemistry of evjite in Dushan (Nanyang, Henan Province): Implication for genesis of Dushan Yu. *Geochim.* **2015**, *44*, 402–412, (In Chinese with English abstract).
8. Jiang, F.J. Analysis of Dushan Jade Petrology feature. *J. Xinyang Norm Univ.* **2007**, *18*, 285–288, (In Chinese with English abstract).
9. Xiao, Q.Y.; Cai, K.Q.; Jiang, F.J. Mineral combinations of diversiform Dushan Jade. *Acta Petrol. Mineral.* **2011**, *30*, 162–168, (In Chinese with English abstract).
10. He, X.M.; Xue, Y.; Jiang, W.Y.; Zhao, H.P. The color mechanism analysis of Dushan jade. *Acta Petrol. Mineral.* **2014**, *33*, 69–75, (In Chinese with English abstract).
11. Liu, J.; Yang, M.X.; Di, J.R.; He, C. Spectra Characterization of the Uvarovite in Anorthitic Jade. *Spectrosc. Spectr. Anal.* **2018**, *38*, 1758–1762, (In Chinese with English abstract).
12. Liu, J.; Yang, M.X.; Di, J.R.; He, C. Mineralogical Characteristic of Dushan Yu Similar. *J. Gems Gemmol.* **2018**, *20*, 26–36, (In Chinese with English abstract).
13. Mohsen, M.-D. Distant vision method. In *Dictionary of Gems and Gemology*, 3rd ed.; Springer: Berlin/Heidelberg, Germany, 2009; p. 271.
14. Mohsen, M.-D. Hydrostatic weighing of specific gravity. In *Dictionary of Gems and Gemology*, 3rd ed.; Springer: Berlin/Heidelberg, Germany, 2009; p. 440.
15. Meng, X.Z.; Zhao, M.F. The legal measurement unit of Vickers hardness and its conversion. *J. Gems Gemmol.* **2007**, *2*, 52.

16. Smith, J.V.; Brown, W.L. Nomenclature, General Properties of Feldspars and Simple Determinative Diagrams. *Feldspar. Miner.* **1988**, 208–228.
17. Grew, E.S.; Mills, S.J.; Galuskina, I.O.; Galuskin, E.V.; Halenius, U. Nomenclature of the garnet supergroup. *Am. Miner.* **2013**, *98*, 785–810. [CrossRef]
18. Leake, B.E.; Woolley, A.R.; Arpes, C.E.S.; Birch, W.D.; Gilbert, M.C.; Grice, J.D.; Hawthorne, F.C.; Kato, A.; Kisch, H.J.; Krivovichev, V.G.; et al. Nomenclature of Amphiboles; Report of the Subcommittee on Amphiboles of the International Mineralogical Association Commission on New Minerals and Mineral Names. *Can. Mineral.* **1997**, *35*, 219–246.
19. Zhang, Y.W.; Cao, J.H.; Liu, Y.; Guo, J.Y. Study on Crystal Chemistry and Spectra of Feldspar from Zhoukoudian Granodiorite. *Spectrosc. Spectr. Anal.* **2009**, *29*, 2480–2484, (In Chinese with English abstract).
20. Matteson, A.; Herron, M.M. End-member feldspar concentrations determined by FTIR spectral analysis. *J. Sediment. Res.* **1993**, *63*, 1144–1148.
21. Wickersheim, K.A.; Lefever, R.A.; Hanking, B.M. Infrared Absorption Spectrum of the Silicate Ion in the Garnet Structure. *J. Chem. Phys.* **1960**, *32*, 271. [CrossRef]
22. Makreski, P.; Runčevski, T.; Jovanovski, G. Minerals from Macedonia. XXVI. Characterization and spectra-structure correlations for grossular and uvarovite. Raman study supported by IR spectroscopy. *J. Raman Spectrosc.* **2011**, *42*, 72–77. [CrossRef]
23. Sharma, S.K.; Simons, B.; Yoder, H.S. Raman study of anorthite, calcium Tschermak's pyroxene, and gehlenite in crystalline and glassy states. *Am. Miner.* **1983**, *68*, 11–12.
24. Le Parc, R.; Champagnon, B.; Dianoux, J.; Jarry, P.; Martinez, V. Anorthite and $CaAl_2Si_2O_8$ glass: Low frequency Raman spectroscopy and neutron scattering. *J. Non-Cryst. Solids.* **2003**, *323*, 155–161. [CrossRef]
25. Prencipe, M.; Mantovani, L.; Tribaudino, M.; Bersani, D.; Lottici, P.P. The Raman spectrum of diopside: A comparison between ab initio calculated and experimentally measured frequencies. *Eur. J. Mineral.* **2012**, *24*, 457–464. [CrossRef]
26. Chopelas, A. Single crystal Raman spectrum of uvarovite, $Ca_3Cr_2Si_3O_{12}$. *Phys. Chem. Miner.* **2006**, *32*, 525–530. [CrossRef]
27. Lenaz, D.; Lughi, V. Raman study of $MgCr_2O_4$–$Fe^{2+}Cr_2O_4$ and $MgCr_2O_4$-$MgFe_2{}^{3+}O_4$ synthetic series: The effects of Fe^{2+} and Fe^{3+} on Raman shifts. *Phys. Chem. Miner.* **2013**, *40*, 491–498. [CrossRef]
28. Kharbish, S. Raman spectroscopic features of Al-Fe^{3+}- poor magnesiochromite and Fe^{2+} - Fe^{3+}- rich ferrian chromite solid solutions. *Mineral. Petrol.* **2018**, *112*, 245–256. [CrossRef]
29. Wopenka, B.; Freeman, J.J.; Nikischer, T. Raman Spectroscopic Identification of Fibrous Natural Zeolites. *Appl. Spectrosc.* **1998**, *52*, 54–63. [CrossRef]
30. Gujar, A.C.; Moye, A.A.; Coghill, P.A.; Teeters, D.C.; Roberts, K.P.; Price, G.L. Raman investigation of the SUZ-4 zeolite. *Microporous Mesoporous Mat.* **2005**, *78*, 131–137. [CrossRef]
31. Buzgar, N.; Apopei, A.I.; Diaconu, V.; Buzatu, A. The composition and source of the raw material of two stone axes of Late Bronze Age from Neamţ County (Romania) - A Raman study. *Univ. Al I Cuza Iasi. Analele Stiint. Geol.* **2013**, *59*, 5–22.
32. Zhang, Q.; Qin, F.; Niu, J.; Wu, X. High-pressure investigation on prehnite: X-ray diffraction and Raman spectroscopy. *High Temp. High Press.* **2018**, *47*, 213–221.
33. Blaha, J.J.; Rosasco, J. Raman microprobe spectra of individual microcrystals and fibers of talc, tremolite, and related silicate minerals. *Anal. Chem.* **2002**, *50*, 892–896. [CrossRef]
34. Wang, C.; Yu, X.; Pan, F.; Chen, H.; Mo, X.; Zhang, J. Raman spectra for structure of tremolite. *J. Chin Ceram. Soc.* **2006**, *34*, 1508–1513.
35. Zhang, C.; Yu, X.Y. Spectral Characteristic and Origin Identification of Tremolite Jade from Sangpiyu, Liaoning Province. *J. Gems Gemmol.* **2018**, *20*, 41–53, (In Chinese with English abstract).
36. Zhang, M.; Saljie, E.K.H.; Redfern, S.A.T.; Bismayer, U.; Groat, L.A. Intermediate structures in radiation damaged titanite ($CaTiSiO_5$): A Raman spectroscopic study. *J. Phys. Condes. Matter.* **2013**, *25*, 1–12. [CrossRef]
37. Liu, S.L.; Bai, B.; He, H.L.; Chu, J.; Sun, Y.P.; Wang, X.; Wang, H.L.; Zhang, M.A. Comparative Study on Influence of High-Pressure Shocking and Radiation Damage on Titanite. *Chin J. High-Press. Phys.* **2019**, 19–26.
38. Liu, S.L.; Bai, B.; Zhang, M.; Sun, Y.P.; Chu, J.; Wang, X.; Wang, H.L. The progress of research on titanite, a host-phase for radioactive nuclides. *Acta Petrol. Mineral.* **2019**, *38*, 259–272.
39. Navas, A.S.; Reddy, B.J.; Fernando, N. Spectroscopic study of chromium, iron, OH, fluid and mineral inclusions in uvarovite and fuchsite. *Spectroc. Acta Pt. A-Molecu. Biomolec. Spectr.* **2004**, *60*, 2261–2268. [CrossRef]
40. Khomenko, V.M.; Platonov, A.N. Electronic absorption spectra of Cr^{3+} ions in natural clinopyroxenes. *Phys. Chem. Miner.* **1985**, *11*, 261–265. [CrossRef]
41. Lin, C.Y.; Zhu, H.B.; Wang, Z.M.; Xie, H.S.; Zhang, Y.M.; Xu, H.G. Optical absorption spectra and colors of jadeites and diopsides. *Acta Mineral. Sin.* **1988**, *3*, 193–199, (In Chinese with English abstract).
42. Taran, M.N.; Ohashi, H.; Langer, K.; Vishnevskyy, A.A. High-pressure electronic absorption spectroscopy of natural and synthetic Cr-bearing clinopyroxenes. *Phys. Chem. Miner.* **2011**, *38*, 345–356. [CrossRef]
43. Cohen, A.J. Anisotropy of absorption bands in some lunar, meteoritic, and terrestrial pyroxenes. *Earth Moon Planets.* **1973**, *7*, 307–321. [CrossRef]
44. Yuan, Y.M.; Qiu, X.J.; Guo, W.S. Optical absorption spectra of diopside. *Acta Mineral. Sin.* **1985**, *2*, 157–184, (In Chinese with English abstract).

45. Rossman, G.R. The optical spectrum of Fe^{3+} and $Fe^{2+} \rightarrow Fe^{3+}$ intervalence charge transfer in jadeite from Burma. *Am. Miner.* **1974**, *59*, 868–870.
46. Proenza, J.; Sole, J.; Melgarejo, J.C. Uvarovite in podiform chromitite; the Moa-Baracoa ophiolitic massif, Cuba. *Can. Mineral.* **1999**, *37*, 679–690.
47. Deer, W.A.; Howie, R.A.; Zussman, J. An Introduction to the Rock-Forming Minerals. *Can. Mineral.* **2013**, *36*, 150–151.
48. Willemse, J.; Bensch, J.J. Inclusions of Original Carbonate Rocks in Gabbro and Norite of the Eastern Part of the Bushveld Complex. *S. Afr. J. Geol.* **1964**, *67*, 1–87.
49. Chakrabo, K.L. Mineralogical note on the chrome-chlorite (kämmererite) and chrome-garnet (uvarovite) from the chromite deposits of Kalrangi, Orissa, India. *Mineral. Mag. J. Miner. Soc.* **1968**, *36*, 962. [CrossRef]
50. Wan, H.M.; Lu, C. Uvarovite and grossular from the Fengtien nephrite deposits, easter Taiwan. *Mineral. Mag.* **1984**, *48*, 31–37. [CrossRef]
51. Mogessie, A.; Rammlmair, D. Occurrence of zoned uvarovite-grossular garnet in a rodingite from the Vumba Schist Belt, Botswana, Africa: Implications for the origin of rodingites. *Mineral. Mag.* **1994**, *58*, 375–386. [CrossRef]
52. Pal, T.; Das, D. Uvarovite from chromite-bearing ultramafic intrusives, Orissa, India, a crystal-chemical characterization using 57Fe Mössbauer spectroscopy. *Am. Miner.* **2010**, *95*, 839–843. [CrossRef]
53. Yu, X.Y. *Colored Gemmology*, 2nd ed.; Geological Publishing House: Beijing, China, 2009; p. 263.
54. Yu, B.S.; Zhao, Z.D.; Su, S.G. *Peteology*, 2nd ed.; Geological Publishing House: Beijing, China, 2012; p. 227.
55. Zhang, J.H.; Li, Z.H.; Wang, X.F. Mineralogical studies of jades from Dushan, Nanyang. *Acta Petrol. Mineral.* **1989**, *8*, 53–64.